

Schwinger Pair Production in Pulsed Electric Fields

Sang Pyo Kim*

*Department of Physics, Kunsan National University, Kunsan 573-701, Korea and
International Center for Relativistic Astrophysics Network,
Piazza della Repubblica, 10 65122 Pescara, Italy*

Hyung Won Lee†

*Institute of Basic Science and Department of Computer Aided Science,
Inje University, 197 Inje-ro, Gimhae 621-749, Korea and
International Center for Relativistic Astrophysics Network,
Piazza della Repubblica, 10 65122 Pescara, Italy*

Remo Ruffini‡

*Dipartimento di Fisica and International Center for Relativistic Astrophysics Network,
Univrsita di Roma “La Sapienza,” Piazzale Aldo Moro 5, I-00185 Roma, Italy and
International Center for Relativistic Astrophysics Network,
Piazza della Repubblica, 10 65122 Pescara, Italy*

(Dated: June 15, 2021)

We numerically investigate the temporal behavior and the structure of longitudinal momentum spectrum and the field polarity effect on pair production in pulsed electric fields in scalar quantum electrodynamics (QED). Using the evolution operator expressed in terms of the particle and antiparticle operators, we find the exact quantum states under the influence of electric pulses and measure the number of pairs of the Minkowski particle and antiparticle. The number of pairs, depending on the configuration of electric pulses, exhibits rich structures in the longitudinal momentum spectrum and undergoes diverse dynamical behaviors at the onset of the interaction but always either converges to a momentum-dependent constant or oscillates around a momentum-dependent time average after the completion of fields.

PACS numbers: 11.15.Tk, 12.20.Ds, 03.65.Fd, 42.50.Xa

I. INTRODUCTION

Schwinger pair production by temporally or spatially inhomogeneous electric fields has been a theoretically and experimentally interesting and challenging issue. The Minkowski or Dirac vacuum under the influence of a strong electric field becomes unstable and emits electron-positron or charged particle-antiparticle pairs. The possibility of directly measuring electron-positron pairs by strong laser sources such as Extreme Light Infrastructure (ELI) has recently boosted intensive researches on pair production by pulsed electric fields [1–4] (for review and references, see also Refs. [5–7]). In contrast to vacuum polarization, pair production has been studied for various electromagnetic configurations, for which many analytical approximation schemes have been elaborated [5].

The Keldysh approach [8, 9] (review and references, see Ref. [10]), the worldline instanton method [11, 12] and the phase-integral or WKB method [13–18], to list a few, have been widely used as analytical approximation schemes. The two typical methods employed to

numerically compute the pair-production rate in time-dependent electric fields are the kinetic approach [19–25] and the Wigner formalism [26–28]. The quantum Vlasov equation has been often used for numerical calculation of pair production with or without back-reaction included [29–36].

The main purpose of this paper is to employ the evolution operator formalism for numerical computation of pair production by pulsed electric fields of various configurations in scalar QED. The stratagem is to express the Hamiltonian in terms of the creation and annihilation operators of the Minkowski vacuum and then find the evolution operator satisfying the time-dependent Schrödinger equation. In fact, the Hamiltonian for a spinless charged boson in a time-dependent electric field in the momentum space consists of infinite number of oscillators with time-dependent frequencies and each oscillator can have the evolution operator represented in $SU(1, 1)$ algebra. We then choose the number operator, the one-pair creation operator and the one-pair annihilation operator in the Minkowski vacuum as the generators for the evolution operator

$$\prod_k e^{\xi_k(t)\hat{a}_k^\dagger\hat{b}_{-k}^\dagger} e^{i\gamma_k(t)(\hat{a}_k^\dagger\hat{a}_k+\hat{b}_{-k}\hat{b}_{-k}^\dagger)} e^{\eta_k(t)\hat{a}_k\hat{b}_{-k}}.$$

In quantum optics the evolution operator for a time-dependent oscillator has been studied in a different representation of $SU(1, 1)$ [37]. The oscillator representation

*Electronic address: sangkim@kunsan.ac.kr

†Electronic address: hwlee@inje.ac.kr

‡Electronic address: ruffini@icra.it

or the creation and annihilation operator representation has also been used to derive the quantum Vlasov equation for pair production [33–36, 38, 39]. The difference of this paper from other earlier works is that we find the evolution operator by directly solving the time-dependent Schrödinger equation, then find the exact quantum state evolved from the Minkowski vacuum, and finally compute the number of pairs during the whole evolution in pulsed electric fields. The evolution operator represented by the creation and annihilation operators has an additional advantage of expressing the exact quantum state as the squeezed vacuum of multi-pairs of particle and antiparticle under the influence of the pulsed electric fields. Further it provides a good measure for counting the number of Minkowski particle and antiparticle pairs.

To study pair production from nontrivial configurations of electromagnetic field, we shall consider only pulsed electric fields, simplified model fields, which act for a finite duration but is uniform over the space. Thus the Minkowski vacuum excites into multi-particle and antiparticle state during the interaction of the electric field and finally settles down in some nontrivial vacuum state and, in an exceptional case, returns to the Minkowski vacuum. The pulsed electric fields to be studied are classified into the mono-polarity type and the di-polarity type. In the first class we consider (i) $E(t) = E_0/\cosh^2(t/\tau)$, (ii) $E(t) = E_0e^{-t^2/\tau^2}$, (iii) $A_{\parallel}(t) = (E_0/\omega)e^{-t^2/\tau^2}\cos(\omega t)$, and in the second class we also consider (iv) $E(t) = E_0/(\cosh^2((t-t_1)/\tau) - E_0/\cosh^2((t-t_2)/\tau))$, (v) $A_{\parallel}(t) = E_0\tau/(1+t^2/\tau^2)$, (vi) $A_{\parallel}(t) = \sqrt{n(n+1)}\tau/\cosh(t/\tau)$.

The electric fields (i)-(vi) provides a good arena to discuss some fundamental questions, not to mention possible applications to ultra-strong lasers. The electric fields (i)-(iii) of mono-polarity type necessarily lead to non-zero gauge potential values, in which the adiabatic basis differs from the Minkowski one. Then a question may be raised whether pairs produced by electric pulses are the Minkowski ones or the adiabatic ones [32, 36]. And the oscillation of the number of pairs after the completion of electric pulses may be another interesting question since the kinetic approach using the adiabatic basis predicts non-oscillating pair production while the nonadiabatic method predicts oscillating pair production for general electric fields except for the solitonic gauge field [36]. The evolution operator provides asymptotic solutions in the remote future for all pulsed electric fields including (i)-(vi), according to which the number of pairs converges to a momentum-dependent constant when the gauge potentials vanish or oscillates around a momentum-dependent time-averaged constant when the gauge potentials have nonzero constant.

Another interesting issue is the structure of the longitudinal momentum spectrum of pairs discovered by Hebenstreit et al in a sinusoidal field with Gaussian envelope [21]. Dumlu and Dunne explained the substructure of the spectrum in the inverse square gauge potential by the Stokes phenomenon, in which more than two pairs of complex turning points for the Fourier mode equation

contribute either in phase or out of phase to the WKB instanton action [16, 17]. The analytical approximation schemes such as the Keldysh approach or the WKB or phase-integral method without Stokes phenomenon cannot explain the substructure of the longitudinal momentum distribution. The evolution operator formalism is efficient enough to compute the longitudinal momentum distribution of produced pairs in the pulsed electric fields (i)-(vi) and confirms the substructure of the spectrum for the critical field strength and Compton time scale. The spectra for (i), (ii), (iv) and (v) exhibit rich structures but those for (iii) and (vi) have relatively simple structure. Bunching of spectrum in the field (iii) is observed around one positive and one negative momentum with the same magnitude. Further the polarity of the electric field (iv) leads to negative momentum dominance or positive momentum dominance in the spectrum.

The organization of this paper is as follows. In Sec. II, we introduce the evolution operator in algebraic form for scalar QED in a pulsed electric field and express the vacuum polarization in terms of the complex parameters for the evolution operator. And we express the number of pairs by the imaginary part of the parameter for the number operator. In Sec. III, by solving the time-dependent Schrödinger equation, we derive a set of first order differential equations for three complex parameters for the evolution operator. And we find the asymptotic solutions for the pulsed electric fields whose gauge potentials approach either zero or nonzero constant after the completion of the interaction. In Sec. IV we give an intuitive interpretation of pair production by pulsed electric fields from the analogy with quantum mechanics. In Sec. V, we numerically investigate pair production by several configurations of electric fields, some of which have recently been studied in literature. In Sec. VI, we discuss the physical implications of the results and conclude the paper.

II. EVOLUTION OPERATOR APPROACH

In scalar QED the Fourier-decomposed Hamiltonian for a spinless charged boson with mass m in an electric field along a fixed direction [36]

$$\begin{aligned}\hat{H}(t) &= \int \frac{d^3k}{(2\pi)^3} \left[\hat{\pi}_k^\dagger \hat{\pi}_k + \omega_k^2(t) \hat{\phi}_k^\dagger \hat{\phi}_k \right], \\ \omega_k^2(t) &= (k_{\parallel} - qA_{\parallel}(t))^2 + \mathbf{k}_{\perp}^2 + m^2,\end{aligned}\quad (1)$$

may have an oscillator representation

$$\hat{H}_k(t) = \frac{1}{2}\Omega_k^{(+)}(t)\hat{N}_k + \frac{1}{2}\Omega_k^{(-)}(t)(\hat{J}_k^{(+)} + \hat{J}_k^{(-)}), \quad (2)$$

where

$$\Omega_k^{(\pm)}(t) = \frac{\omega_k^2(t) \pm \omega_k^2(t_0)}{\omega_k(t_0)}, \quad (3)$$

and

$$\hat{N}_k = \hat{a}_k^\dagger \hat{a}_k + \hat{b}_{-k} \hat{b}_{-k}^\dagger, \quad \hat{J}_k^{(+)} = \hat{a}_k^\dagger \hat{b}_{-k}^\dagger, \quad \hat{J}_k^{(-)} = \hat{a}_k \hat{b}_{-k}. \quad (4)$$

Here we have used the oscillator representation in the Minkowski vacuum

$$\begin{aligned} \hat{\phi}_k &= \frac{1}{\sqrt{2\omega_k(t_0)}} (\hat{a}_k + \hat{b}_{-k}^\dagger), \\ \hat{\pi}_k &= i\sqrt{\frac{\omega_k(t_0)}{2}} (\hat{a}_k^\dagger - \hat{b}_{-k}), \end{aligned} \quad (5)$$

where \hat{a}_k and \hat{b}_{-k}^\dagger are the particle and antiparticle operators. And these operators constitute the $SU(1, 1)$ algebra

$$[\hat{N}_k, \hat{J}_k^{(\pm)}] = \pm 2\hat{J}_k^{(\pm)}, \quad [\hat{J}_k^{(+)}, \hat{J}_k^{(-)}] = \hat{N}_k. \quad (6)$$

In this paper we shall focus on pulsed electric fields that act effectively for a finite duration. Before the onset of a pulsed electric field, we may choose a gauge

$$A_{\parallel}(t) = 0, \quad E(t) = 0 \quad (t \leq t_0), \quad (7)$$

so that the in-vacuum is the Minkowski vacuum. The constant electric field with $A_{\parallel} = -E_0 t$ will not be considered in this paper since no gauge can be chosen to make the initial vacuum the Minkowski one, for which the in- and out-vacua are defined as asymptotic states.

The evolution of the Minkowski vacuum follows the time-dependent Schrödinger equation

$$i \frac{\partial \hat{U}_k(t)}{\partial t} = \hat{H}_k(t) \hat{U}_k(t). \quad (8)$$

The evolution operator in time-ordered integral

$$\hat{U}_k(t) = \mathbb{T} \left(e^{-i \int_{t_0}^t \hat{H}_k(t') dt'} \right), \quad (9)$$

does not provide useful information about the quantum state unless $\Omega_k^{(-)}(t) = 0$ since the Hamiltonian is then entangled such that $[\hat{H}_k(t''), \hat{H}_k(t')] \neq 0$ for $t'' \neq t'$. The particle and antiparticle operators evolve as

$$\begin{aligned} \hat{a}_k(t) &= \hat{U}_k(t) \hat{a}_k \hat{U}_k^\dagger(t) := \mu_k(t) \hat{a}_k + \nu_k^* \hat{b}_{-k}^\dagger, \\ \hat{b}_{-k}(t) &= \hat{U}_k(t) \hat{b}_{-k} \hat{U}_k^\dagger(t) := \mu_k(t) \hat{b}_{-k} + \nu_k^* \hat{a}_k^\dagger. \end{aligned} \quad (10)$$

The time-dependent vacuum state is given by

$$|0, t\rangle = \prod_k \hat{U}_k(t) |0, \text{in}\rangle, \quad (11)$$

where $|0, \text{in}\rangle$ denotes the Minkowski vacuum. The number of the Minkowski particle carried by the time-dependent vacuum, which is equal to the number of time-dependent particle carried by the Minkowski vacuum, is

$$\langle 0, t | \hat{a}_k^\dagger \hat{a}_k | 0, t \rangle = \langle 0, \text{in} | \hat{a}_k^\dagger(t) \hat{a}_k(t) | 0, \text{in} \rangle = |\nu_k|^2. \quad (12)$$

The same is true for the antiparticle production. Further, the vacuum persistence is related to the mean number [40]

$$|\langle 0, t | 0, \text{in} \rangle|^2 = \exp \left[- \sum_k \ln(1 + |\nu_k|^2) \right] \quad (13)$$

On the other hand, the $SU(1, 1)$ algebra may lead to the evolution operator of the form

$$\hat{U}_k(t) = e^{\xi_k(t) \hat{J}_k^{(+)}} e^{i\gamma_k(t) \hat{N}_k} e^{\eta_k(t) \hat{J}_k^{(-)}}. \quad (14)$$

Here the complex parameters ξ_k , γ_k and η_k will be determined from the evolution equation (8). It should be mentioned that Eq. (14) differs from Eq. (31) of Ref. [37] for a time-dependent oscillator, which would read

$$\begin{aligned} \hat{J}_k^{(+)} &= i\hat{\phi}_k^\dagger \hat{\phi}_k, \quad \hat{J}_k^{(-)} = i\hat{\pi}_k^\dagger \hat{\pi}_k, \\ \hat{J}_k^{(0)} &= \frac{i}{4} (\hat{\pi}_k \hat{\phi}_k + \hat{\phi}_k \hat{\pi}_k + \hat{\pi}_k^\dagger \hat{\phi}_k^\dagger + \hat{\phi}_k^\dagger \hat{\pi}_k^\dagger). \end{aligned} \quad (15)$$

Another form of the evolution operator is realized by inverting the Bogoliubov transformation (10) in Ref. [40]. The representation (8) is particularly useful for pair production since it expresses the out-vacuum as a squeezed vacuum of the Minkowski vacuum

$$\begin{aligned} |0, t\rangle &= \prod_k e^{i\gamma_k(t)} e^{\xi_k(t) \hat{J}_k^{(+)}} |0, \text{in}\rangle \\ &= \prod_k e^{i\gamma_k(t)} \left(\sum_{n=0}^{\infty} \xi_k^n(t) |n_k, \bar{n}_{-k}, \text{in}\rangle \right), \end{aligned} \quad (16)$$

where n_k and \bar{n}_{-k} denote the n particles with momentum k and n antiparticles with momentum $-k$, respectively. Thus pair production conserves charge and momentum. It further leads to the vacuum polarization

$$\langle 0, t | 0, \text{in} \rangle = \exp \left[-i \sum_k \gamma_k^*(t) \right], \quad (17)$$

and the vacuum persistence

$$|\langle 0, t | 0, \text{in} \rangle|^2 = \exp \left[-2 \sum_k \gamma_{\text{Im}k}(t) \right], \quad (18)$$

where $\gamma_{\text{Im}k}$ denotes the imaginary part of γ_k . Therefore we can find the number of produced pairs from the imaginary part of the parameter $\gamma_k(t)$ during the interaction of the electric field as well as after the completion of the interaction

$$|\nu_k(t)|^2 = e^{2\gamma_{\text{Im}k}(t)} - 1. \quad (19)$$

III. MASTER EQUATIONS FOR EVOLUTION OPERATOR

The time-dependent Schrödinger equation (8) together with $SU(1, 1)$ algebra leads to the differential equations

for the complex parameters ¹

$$\dot{\gamma}_k + i\dot{\eta}_k e^{-2i\gamma_k} \xi_k = -\frac{1}{2}\Omega_k^{(+)}, \quad (20)$$

$$\dot{\xi}_k - 2i\dot{\gamma}_k \xi_k + \dot{\eta}_k e^{-2i\gamma_k} \xi_k^2 = -\frac{i}{2}\Omega_k^{(-)}, \quad (21)$$

$$\dot{\eta}_k e^{-2i\gamma_k} = -\frac{i}{2}\Omega_k^{(-)}. \quad (22)$$

The differential equations for the real and imaginary parts of complex parameters can be grouped into the set that determines pair production

$$\dot{\gamma}_{Ik} = -\frac{1}{2}\Omega_k^{(-)}\xi_{Ik}, \quad (23)$$

$$\dot{\xi}_{Rk} = \Omega_k^{(+)}\xi_{Ik} + \Omega_k^{(-)}\xi_{Rk}\xi_{Ik}, \quad (24)$$

$$\dot{\xi}_{Ik} = -\Omega_k^{(+)}\xi_{Rk} - \frac{1}{2}\Omega_k^{(-)}(1 + \xi_{Rk}^2 - \xi_{Ik}^2), \quad (25)$$

and into another set that are relevant for the vacuum polarization

$$\dot{\gamma}_{Rk} = -\frac{1}{2}\Omega_k^{(+)} - \frac{1}{2}\Omega_k^{(-)}\xi_{Rk}, \quad (26)$$

$$\dot{\eta}_{Rk} = \frac{1}{2}\Omega_k^{(-)}e^{-2\gamma_{Ik}} \sin(\gamma_{Rk}), \quad (27)$$

$$\dot{\eta}_{Ik} = -\frac{1}{2}\Omega_k^{(-)}e^{-2\gamma_{Ik}} \cos(\gamma_{Rk}). \quad (28)$$

To get the initial data for the parameters, we employ the Baker-Campbell-Hausdorff formula to write the evolution in a single exponential operator

$$\begin{aligned} \hat{U}_k(t) = \exp & \left[(1 - i\gamma_k(t))(\xi_k(t)\hat{J}_k^{(+)} + \eta_k(t)\hat{J}_k^{(-)}) \right. \\ & \left. + \left(i\gamma_k(t) + \frac{1}{2}\xi_k(t)\eta_k(t)(1 - i\gamma_k(t)) \right) \hat{N}_k + \dots \right], \quad (29) \end{aligned}$$

where the dots denote polynomials of ξ_k , γ_k and η_k higher than third order. Before the onset of the electric field $\Omega_k^{(-)} = 0$, the evolution operator takes the form

$$\hat{U}_k(t) = e^{-\frac{i}{2}\Omega_k(t_0)\hat{N}_k(t-t_0)}. \quad (30)$$

Therefore the initial data are given by

$$\xi(t_0) = \gamma_k(t_0) = \eta(t_0) = 0, \quad \dot{\gamma}_k(t_0) = -\frac{1}{2}\Omega_k(t_0). \quad (31)$$

For pulsed electric fields such that $E(t) = 0$ and $A_{\parallel}(t) = \text{constant}$ for large t , we find the asymptotic solutions. In the first case of $A_{\parallel}(\infty) = 0$ so that $\Omega_k^{(-)}(\infty) = 0$

and $\Omega_k^{(+)}(\infty) = 2\omega_k(t_0) = 2\omega_k(\infty)$, the asymptotic solutions are

$$\begin{aligned} \gamma_{Ik}(t) &= \gamma_{Ik}(\infty), \\ \xi_{Rk}(t) &= |\xi_k(\infty)| \cos(2\omega_k(\infty)t + \varphi_k), \\ \xi_{Ik}(t) &= -|\xi_k(\infty)| \sin(2\omega_k(\infty)t + \varphi_k). \quad (32) \end{aligned}$$

Here three integration constants are φ_k and the remaining two are identified with those at $t = \infty$. This implies that the number of pairs per unit volume and per unit time approaches constant and the squeezing parameter rotates as $\xi_k = |\xi_k(\infty)|e^{-i(2\omega_k(\infty)t + \varphi_k)}$. In the second case of more general $A_{\parallel}(\infty) \neq 0$ and $\Omega_k^{(-)}(\infty) \neq 0$, the asymptotic solutions are given by

$$\begin{aligned} \gamma_{Ik}(t) &= c_1 - \frac{1}{2}\Omega_k^{(-)}(\infty) \int^t \xi_{Ik} dt', \\ \xi_{Ik}(t) &= -\frac{2\omega_k(\infty)}{\Omega_k^{(-)}(\infty) c_2 + \sqrt{1 + c_3^2} \cos(2\omega_k(\infty)t + \vartheta_k)}, \\ \xi_{Rk}(t) &= -\frac{\Omega_k^{(+)}(\infty)}{\Omega_k^{(-)}(\infty)} \left[1 - \left(1 - 2\frac{\Omega_k^{(-)}(\infty)}{(\Omega_k^{(+)}(\infty))^2} \dot{\xi}_{Ik} \right. \right. \\ & \quad \left. \left. - \frac{(\Omega_k^{(-)}(\infty))^2}{(\Omega_k^{(+)}(\infty))^2} (1 - (\xi_{Ik})^2) \right)^{1/2} \right], \quad (33) \end{aligned}$$

where c_1 , c_2 and c_3 are integration constants and $\tan \vartheta_k = 1/c_3$. Further integrating Eq. (33)

$$\gamma_{Ik}(t) = c_1 + \frac{1}{2} \ln \left| c_2 + \sqrt{1 + c_3^2} \sin(2\omega_k(\infty)t + \vartheta_k) \right|, \quad (34)$$

we find the number of produced pairs

$$N_k(t) = e^{2c_1} \left| c_2 + \sqrt{1 + c_3^2} \sin(2\omega_k(\infty)t + \vartheta_k) \right| - 1. \quad (35)$$

The integration constants of the asymptotic solutions (32) or (33) should be determined by solving the evolution equations (23)-(25) or may be found from other analytical methods.

IV. SCATTERING PICTURE

The general feature of pair production can be understood from the analogy with quantum mechanical scattering problem. We write the mode equation for the scalar field as

$$-\frac{d^2 \phi_k}{dt^2} - P_{\parallel}^2(t) \phi_k = (m^2 + \mathbf{k}_{\perp}^2) \phi_k, \quad (36)$$

where the kinematic momentum is

$$P_{\parallel}(t) = k_{\parallel} - qA_{\parallel}(t). \quad (37)$$

The mode equation (36) in the domain of time can be interpreted as a nonrelativistic particle with mass 1/2 and energy $\epsilon = m^2 + \mathbf{k}_{\perp}^2$ under the potential $V(t) =$

¹ Here we have used the algebraic relation, $e^{\lambda \hat{N}} \hat{M} e^{-\lambda \hat{N}} = \sum_{n=0}^{\infty} \frac{\lambda^n}{n!} [\hat{N}, \hat{M}]^{(n)}$, where $[\hat{N}, \hat{M}]^{(0)} = \hat{M}$ and $[\hat{N}, \hat{M}]^{(n)} = [\hat{N}, [\hat{N}, \hat{M}]^{(n-1)}]$.

$-P_{\parallel}^2(t)$. We assume that the pulsed electric field has the gauge potential $A_{\parallel}(-\infty) = 0$ but $A_{\parallel}(\infty) = \text{constant}$. Depending on the profile of $A_{\parallel}(t)$ during the interaction of the electric field pulse, the potential becomes a barrier or well and the asymptotic value $V(\infty)$ may be the same as $V(-\infty)$ or higher (the green line) or lower (the sky blue line) (see Fig. 1). The incident wave from the future is partially reflected by the well or barrier back into the future and partially transmitted into the past

$$\alpha_k v_k(t) + \beta_k v_k^*(t) \longleftrightarrow u_k(t), \quad (38)$$

where

$$u_k(t) = \frac{e^{-i\omega_k(-\infty)t}}{\sqrt{2\omega_k(-\infty)}}, \quad v_k(t) = \frac{e^{-i\omega_k(\infty)t}}{\sqrt{2\omega_k(\infty)}}. \quad (39)$$

First, in the limit of weak field ($|qA_{\parallel}| \ll m$) or large momentum such that

$$\left| \frac{\omega_k(t) - \omega_k(-\infty)}{\omega_k(-\infty)} \right| \ll 1, \quad (40)$$

Eq. (36) is the scattering by a high energy particle over a shallow well or barrier. Thus the reflection coefficient β_k is suppressed for all k_{\parallel} . Second, in the limit of strong field ($|qA_{\parallel}| \gg m$) or small momentum such that

$$\left| \frac{\omega_k(t) - \omega_k(-\infty)}{\omega_k(-\infty)} \right| \geq 1, \quad (41)$$

Eq. (36) is the scattering over a relatively deep well or high barrier. The kinetic energy for small k_{\parallel} is smaller than for large k_{\parallel} , which means that the reflection coefficient for small k_{\parallel} is larger than that for large k_{\parallel} .

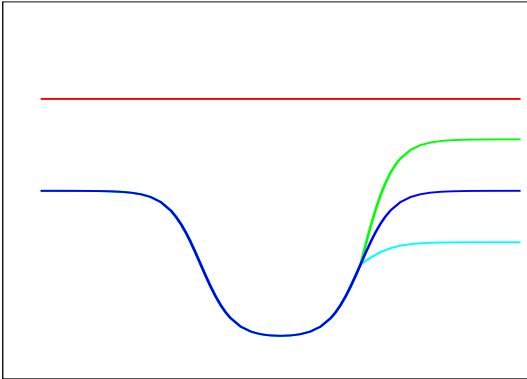


FIG. 1: (color online). The schematic plot for the scattering problem: the red line denotes the energy of the particle, $\mu^2 = m^2 + \mathbf{k}_{\perp}^2$; the blue line denotes a potential, $V(t) = -P_{\parallel}^2(t)$, where $A_{\parallel}(\mp\infty) = 0$; the green or sky blue line denote a potential, $V(t) = -P_{\parallel}^2(t)$, where $A_{\parallel}(-\infty) = 0$ but $A_{\parallel}(\infty) \neq 0$.

The above quantum mechanical interpretation may have a direct interpretation of pair production when $A_{\parallel}(\infty) = 0$ so that $\omega_k(\infty) = \omega_k(-\infty)$. The positive frequency solution in the right hand side of Eq. (38) splits

into a positive solution and a negative solution with the same frequency in the left hand side. Thus $|\beta_k|^2$ is the mean number of produced pairs by the electric field pulse. However, when $A_{\parallel}(\infty) \neq 0$ and $\omega_k(\infty) \neq \omega_k(-\infty)$, we may write the solution in the future by another basis with the initial frequency

$$\phi_k(t) = \mu_k u_k(t) + \nu_k u_k^*(t). \quad (42)$$

Using the Wronskian

$$\text{Wr}[u_k, u_k^*] = i, \quad \text{Wr}[v_k, v_k^*] = i, \quad (43)$$

we find the relation between two set of coefficients

$$\begin{aligned} \mu_k &= -i \left(\alpha_k \text{Wr}[v_k, u_k^*] + \beta_k \text{Wr}[v_k^*, u_k^*] \right), \\ \nu_k &= i \left(\alpha_k \text{Wr}[v_k, u_k] + \beta_k \text{Wr}[v_k^*, u_k] \right). \end{aligned} \quad (44)$$

Thus the number of produced pairs measured with respect to the Minkowski vacuum

$$\begin{aligned} |\mu_k(t)|^2 &= \left| \frac{1}{2} \left(\sqrt{\frac{\omega_k(\infty)}{\omega_k(-\infty)}} - \sqrt{\frac{\omega_k(-\infty)}{\omega_k(\infty)}} \right) \alpha_k \right. \\ &\quad \left. + \frac{1}{2} \left(\sqrt{\frac{\omega_k(\infty)}{\omega_k(-\infty)}} + \sqrt{\frac{\omega_k(-\infty)}{\omega_k(\infty)}} \right) \beta_k e^{2i\omega_k(\infty)t} \right|^2, \end{aligned} \quad (45)$$

oscillates with the frequency $2\omega_k(\infty)$ unless $\omega_k(\infty) = \omega_k(-\infty)$, which confirms the the result (35) from the asymptotic solution. Note that $|\nu_k(t)|^2$ counted with respect to the Minkowski vacuum is the same as $|\beta_k(t)|^2$ counted with respect to the adiabatic vacuum only when $\omega_k(\infty) = \omega_k(-\infty)$. (For discussion on pair production in the adiabatic basis in QED, see Ref. [32].)

A few remarks are in order. First, the kinetic approach

$$\begin{aligned} \phi_k(t) &= \bar{\alpha}_k(t) \frac{e^{-i \int_{-\infty}^t \omega_k(t') dt'}}{\sqrt{2\omega_k(t)}} + \bar{\beta}_k(t) \frac{e^{i \int_{-\infty}^t \omega_k(t') dt'}}{\sqrt{2\omega_k(t)}}, \\ \dot{\phi}_k(t) &= -i\omega_k(t) \\ &\times \left(\bar{\alpha}_k(t) \frac{e^{-i \int_{-\infty}^t \omega_k(t') dt'}}{\sqrt{2\omega_k(t)}} - \bar{\beta}_k(t) \frac{e^{i \int_{-\infty}^t \omega_k(t') dt'}}{\sqrt{2\omega_k(t)}} \right) \end{aligned} \quad (46)$$

applied to the pulsed electric field results in the asymptotic solutions (38) with the coefficients

$$\begin{aligned} \alpha_k(\infty) &= \bar{\alpha}_k(\infty) e^{-i \int_{-\infty}^{t_1} \omega_k(t') dt' + i\omega_k(\infty)t_1}, \\ \beta_k(\infty) &= \bar{\beta}_k(\infty) e^{i \int_{-\infty}^{t_1} \omega_k(t') dt' - i\omega_k(\infty)t_1}. \end{aligned} \quad (47)$$

where t_1 is an arbitrary time beyond which $\omega_k(t) = \omega_k(\infty)$. Thus the number of pairs from the kinetic approach is the same from Eq. (38), that is, $|\beta_k|^2 = |\bar{\beta}_k|^2$. Second, some gauge potential may involve an odd function $\bar{A}_{\parallel}(t)$ such that for a fixed constant c

$$P_{\parallel}(t) = k_{\parallel} + c - \bar{A}_{\parallel}(t), \quad (48)$$

and $P_{\parallel}(-t)$ for $k_{\parallel}+c$ is the negative of $P_{\parallel}(t)$ for $-(k_{\parallel}+c)$. This implies that the scattering equation for $-(k_{\parallel}+c)$ is the backward scattering for $(k_{\parallel}+c)$ in time and has the same reflection and transmission coefficients. Thus the number of pairs is symmetric in the longitudinal momentum around $k_{\parallel} = -c$ in the remote future.

V. PAIR PRODUCTION IN MONO-POLARITY ELECTRIC FIELDS

For the purpose of numerical calculations, we use the Compton unit $\hbar = c = e = m = 1$ so that the time is measured in Compton time, the field strength in the critical strength and the energy in the rest mass energy of the particle:

$$t_C = \frac{\hbar}{mc^2} = 1, \quad E_c = \frac{m^2 c^3}{\hbar e} = 1, \quad mc^2 = 1. \quad (49)$$

We restrict to the zero-transverse momentum, which is equivalent to replacing $m^2 = 1$ by $\epsilon_{\perp}^2 = m^2 + \mathbf{k}_{\perp}^2 = 1$ in all the calculations below. In this unit system $\Omega_k^{(\pm)}$ in Eqs. (23)-(25) read

$$\begin{aligned} \Omega_k^{(+)}(t) &= \frac{2 + P_{\parallel}^2(t) + k_{\parallel}^2}{\sqrt{1 + k_{\parallel}^2}}, \\ \Omega_k^{(-)}(t) &= \frac{P_{\parallel}^2(t) - k_{\parallel}^2}{\sqrt{1 + k_{\parallel}^2}}. \end{aligned} \quad (50)$$

Further we shall consider only the strong field regime since pair production is prominent for an electric field near or above the critical strength and dynamical characteristics is manifest at the Compton time scale.

$$\text{A. } E(t) = \frac{E_0}{\cosh^2(\frac{t}{\tau})}$$

The Sauter electric field is a frequently used model in QED which is uniform in space but nontrivial in time. The Green function and the asymptotic number of pairs of the adiabatic particle and antiparticle have been known [41]. The gauge potential is chosen

$$A_{\parallel}(t) = -E_0\tau \left(1 + \tanh\left(\frac{t-10\tau}{\tau}\right)\right), \quad (51)$$

such that the initial state is the Minkowski vacuum. The duration of the field is effectively characterized by 2τ . We shift the peak of electric field by 10τ only for the numerical purpose.

At the critical strength $E_0 = 1$ for a Compton time scale pulse $\tau = 1$, the number of pairs is order of one and exhibits both the temporal behavior and the substructure of the longitudinal momentum spectrum as shown in Fig. 2. The pair production for small momentum in the

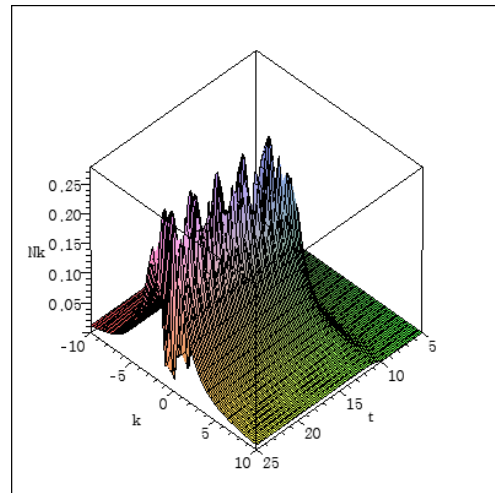


FIG. 2: (color online). The number of pairs for the Sauter electric field with $E_0 = 1$ and $\tau = 1$ is plotted as a function of time and longitudinal momentum.

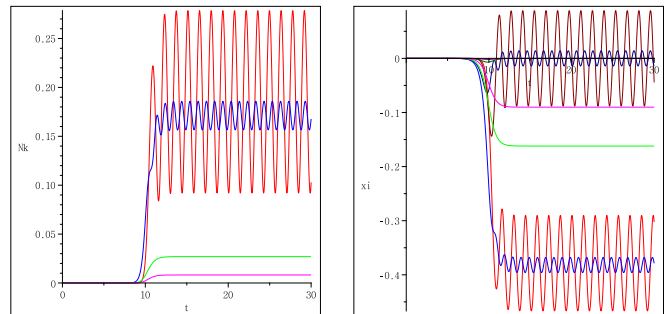


FIG. 3: (color online). For the Sauter electric field, the number of pairs $N_k(t)$ [left panel] and the real and imaginary parts of the function $\xi_k(t)$ [right panel] are plotted as a function of time for $k_{\parallel} = 0$ (red), $k_{\parallel} = 1$ (blue), $k_{\parallel} = 5$ (green), and $k_{\parallel} = 10$ (magenta), where the real part is in the light color and the imaginary part is in the dark color.

Compton unit begins to oscillate around the time of interaction as shown in detail in Fig. 3, in which the gauge potential at $t = 10$ is the half of the asymptotic value in the remote future. The pair production increases soon after the electric field is turned on, reaches the maximum within a few Compton times and then oscillates with large amplitude for small k_{\parallel} and with small amplitude for large k_{\parallel} . The small amplitude oscillation for large k_{\parallel} is not shown in Fig. 2 and in the left panel of Fig. 3 due to a different order of magnitude. However, the asymptotic solutions (33) predict oscillations for all k_{\parallel} since $A_{\parallel}(\infty) \neq 0$, which is numerically confirmed. The time-averaged number of pairs monotonically decreases as the momentum increases.

The suppression of pair production for large momentum is expected from the scattering picture in Sec. IV, according to which the particle has a large kinetic energy compared to the potential well or barrier and thus

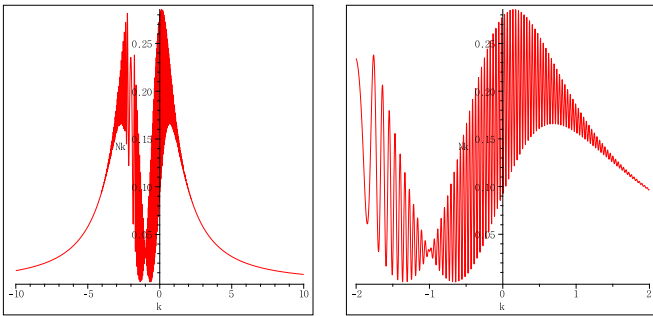


FIG. 4: (color online). For the Sauter electric field, the longitudinal momentum spectrum of pairs at the time $t = 100$ is plotted as a function of momentum in the range of $-10 \leq k_{\parallel} \leq 10$ [left panel] and magnified in the range of $-2 \leq k_{\parallel} \leq 2$ [right panel].

has a small reflection coefficient, implying small pair production. The oscillatory and temporal behavior of the squeezed vacuum (16) can be understood from ξ_k in the right panel of Fig. 3, in which it oscillates with large amplitude for small momentum while it oscillates with small amplitude for large momentum, according to the asymptotic solutions (33).

The longitudinal momentum spectrum of pairs shows a substructure, which could not be seen by the number of adiabatic pairs [41]. Since the kinematic momentum $P_{\parallel}(t)$ for $k_{\parallel} + 1$ and $-(k_{\parallel} + 1)$ is antisymmetric in time, the longitudinal momentum spectrum of number of pairs is symmetric around $k_{\parallel} = -1$ according to Sec. IV, which is numerically confirmed in Fig. 4. Pairs are minimally produced for $k_{\parallel} = -1$, for which $P_{\parallel}(-t) = -P_{\parallel}(t)$ and $\omega_k(-\infty) = \omega_k(\infty)$. The pair production is suppressed for large momentum as expected.

$$\text{B. } E(t) = E_0 e^{-\frac{t^2}{\tau^2}}$$

The gauge potential given by the error-function

$$\begin{aligned} A_{\parallel}(t) &= -E_0 \left(\frac{\sqrt{\pi}\tau}{2} + \int_0^{t-10\tau} e^{-\frac{t'^2}{\tau^2}} dt' \right) \\ &= -\frac{\sqrt{\pi}E_0\tau}{2} \left\{ 1 + \text{erf} \left(\frac{t-10\tau}{\tau} \right) \right\}, \end{aligned} \quad (52)$$

leads to the Gaussian electric field

$$E(t) = E_0 e^{-\frac{(t-10\tau)^2}{\tau^2}}. \quad (53)$$

The center of the Gaussian field is shifted for the numerical purpose. The Gaussian electric field decays more rapidly and thus produces relatively smaller pairs than the Sauter electric field in Sec. V A. For the numerical work we set $E_0 = 1$ and $\tau = 1$ as for the Sauter electric field.

The number of pairs as function of time and longitudinal momentum in Fig. 5 exhibits a similar structure as

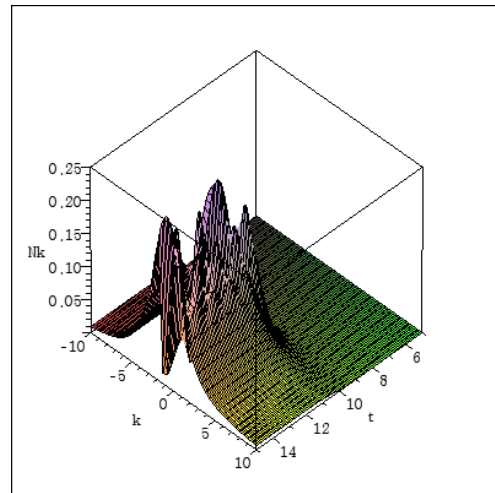


FIG. 5: (color online). The number of pairs in the Gaussian electric field with $E_0 = 1$ and $\tau = 1$ is plotted as a function of time and longitudinal momentum.

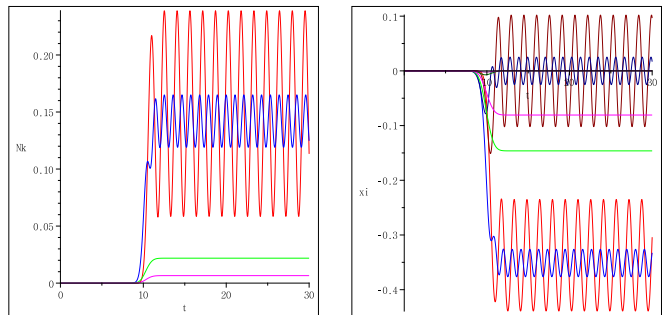


FIG. 6: (color online). For the Gaussian electric field, the number of pairs $N_k(t)$ [left panel] and the real and imaginary parts of the function $\xi_k(t)$ [right panel] are plotted as a function of time for $k_{\parallel} = 0$ (red), $k_{\parallel} = 1$ (blue), $k_{\parallel} = 5$ (green), and $k_{\parallel} = 10$ (magenta), where the real part is in the light color and the imaginary part is in the dark color.

that of the Sauter field in Fig. 2. It has a structure for small momentum but it is suppressed for large momentum. The similarity of the temporal behavior can be seen by comparing the left panel of Fig. 6 with Fig. 3. The longitudinal momentum spectrum of pairs in Fig. 7 also has a similar pattern as Fig. 4. As the error-function is an odd function $\text{erf}(-t) = -\text{erf}(t)$, it is symmetric around $k_{\parallel} = -\sqrt{\pi}/2$ according to Sec. IV, which is numerically confirmed in Fig. 7. Note that $k_{\parallel} = -\sqrt{\pi}/2$ is the channel for minimal pair production for small momentum. The suppression of pair production for large momentum is also shown in Fig. 7.

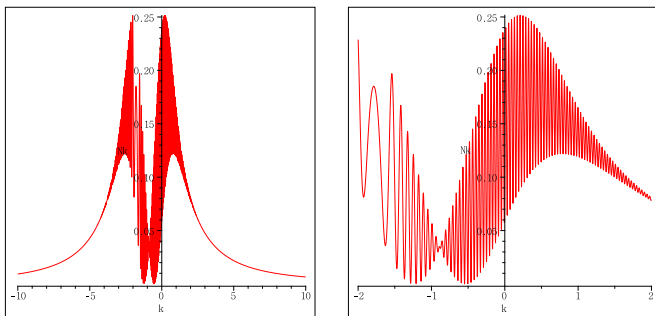


FIG. 7: (color online). For the Gaussian electric field, the longitudinal momentum spectrum of pairs at $t = 100$ is plotted in the range of $-10 \leq k_{\parallel} \leq 10$ [left panel] and magnified in the range of $-2 \leq k_{\parallel} \leq 2$ [right panel].

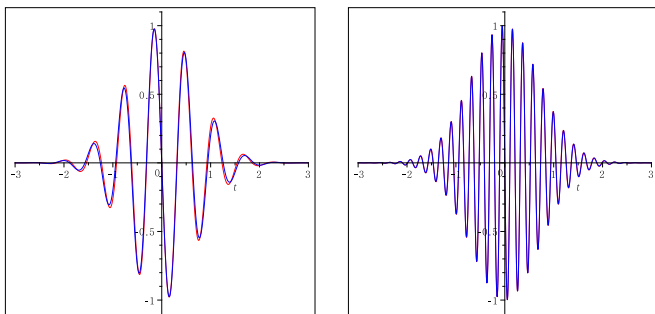


FIG. 8: (color online). The profile of electric field (55) is plotted in red color for $E_0 = 1$, $\tau = 1$ and $\omega = 10$ [left panel] and $\omega = 30$ [right panel]. The curve in blue color in each panel is $e^{-(t-10)^2} \sin(\omega t)$ for the same value of ω .

$$\text{C. } A_{\parallel}(t) = \frac{E_0}{\omega} e^{-\frac{t^2}{\tau^2}} \cos(\omega t)$$

Finally, we consider a gauge potential

$$A_{\parallel}(t) = \frac{E_0}{\omega} e^{-\frac{(t-10\tau)^2}{\tau^2}} \cos(\omega t), \quad (54)$$

which leads to the oscillating Gaussian electric field

$$E(t) = E_0 e^{-\frac{(t-10\tau)^2}{\tau^2}} \sin(\omega t) + \frac{2E_0}{\omega\tau} \left(\frac{t-10\tau}{\tau} \right) e^{-\frac{(t-10\tau)^2}{\tau^2}} \cos(\omega t). \quad (55)$$

As shown in Fig.8 the first term is dominant in the region $|t - 10\tau| \leq 2/(\omega\tau^2)$ and oscillates with an Gaussian envelope $e^{-(t-10\tau)^2/\tau^2}$ and beyond that region the second term has a linearly growing factor but both terms are exponentially suppressed.

For the numerical work we set $E_0 = 1$, $\tau = 1$ and $\omega = 10$ or $\omega = 30$. It is surprising that the number of pairs in Fig.9 is bunched around $k_{\parallel} = -5$ and $k_{\parallel} = 5$. The longitudinal momentum spectrum in Fig.10 shows bunching with momentum separation of 10 and 30 for $\omega = 10$ and $\omega = 30$, respectively. And the rapidly oscillating factor suppresses pair production, though the peak

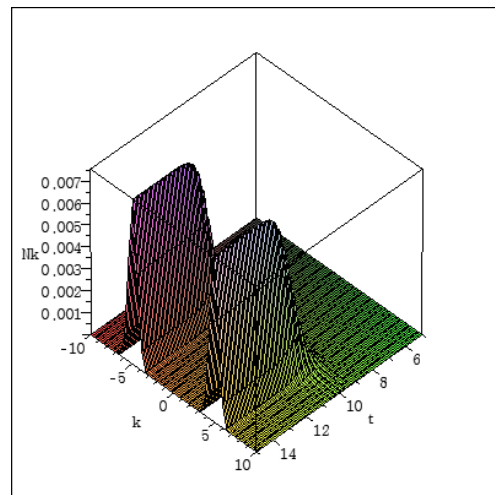


FIG. 9: (color online). The number of pairs in the oscillating Gaussian electric field with $E_0 = 1$ and $\tau = 1$ is plotted as a function of time and longitudinal momentum.

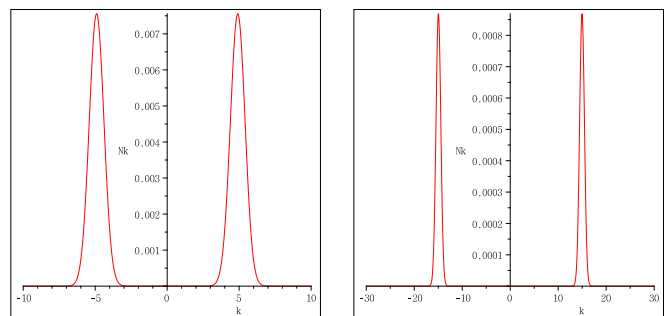


FIG. 10: (color online). For the oscillating Gaussian electric field, the longitudinal momentum spectrum of pairs is plotted at $t = 100$ for $\omega = 10$ [left panel] and $\omega = 30$ [right panel].

intensity in Fig.8 is almost comparable to the Sauter electric field in Sec.V A and the Gaussian electric field in Sec.V B. The numerical study also shows a similar pattern in pair production and bunching of pairs in the gauge potential

$$A_{\parallel}(t) = \frac{E_0}{\omega} e^{-\frac{(t-10\tau)^2}{\tau^2}} \sin(\omega t). \quad (56)$$

VI. PAIR PRODUCTION IN DI-POLARITY ELECTRIC FIELDS

In this section we study how the polarity of the electric field influences pair production, in particular, when the electric field changes the polarity during the interaction. It is interesting to understand how the produced pairs behave when another electric pulse of opposite polarity acts. Do they annihilate each other partially or completely? Or are there more pairs produced by the second pulse? In order to answer some of these questions we consider three model fields.

$$\text{A. } E(t) = \frac{E_0}{\cosh^2(\frac{t-t_1}{\tau})} - \frac{E_0}{\cosh^2(\frac{t-t_2}{\tau})}$$

As the first model we consider the di-polarity Sauter electric field, two Sauter electric fields acting with a time lag and in opposite directions. The model gauge field is given by

$$A_{\parallel} = -E_0\tau \left(\tanh\left(\frac{t-10\tau}{\tau}\right) - \tanh\left(\frac{t-20\tau}{\tau}\right) \right). \quad (57)$$

Though we cannot exactly solve QED problem in this gauge potential, we may understand the characteristic feature of pair production by each of Sauter electric fields when they are separated by a sufficient time gap as in quantum mechanics.

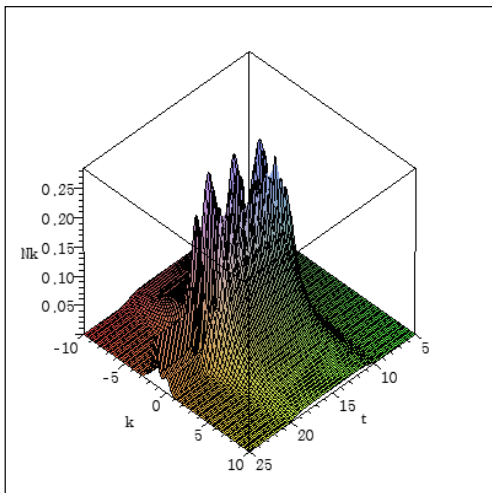


FIG. 11: (color online). The number of pairs in the di-polarity Sauter electric field with $E_0 = 1$ and $\tau = 1$ is plotted as a function of time and longitudinal momentum.

For the numerical work we set $E_0 = 1$ and $\tau = 1$ so that two Sauter electric pulses are effectively separated. At the onset of the interaction the peak of number of pairs in Fig. 11 is almost the same as the single Sauter electric field in Fig. 2, though it exhibits more structure. However, the main difference appears after the completion of the interaction. The di-polarity Sauter electric field returns to the Minkowski vacuum while the Sauter electric field has a constant residual gauge and $\omega_k(-\infty) \neq \omega_k(\infty)$. The asymptotic solutions (32) predict that the number of pairs for the di-polarity Sauter field approaches to a constant, as shown in Figs. 11 and 12, while Eq. (35) predicts that the number of pairs for the Sauter field oscillates with a constant amplitude around the time-averaged value, as shown in Figs. 2 and 3.

The gauge potential in between two peaks of the di-polarity Sauter field has approximately the shape of square potential barrier, in which pair production oscillates according to the asymptotic solution (35). No pair production for $k_{\parallel} = 0$ is the numerical coincidence that

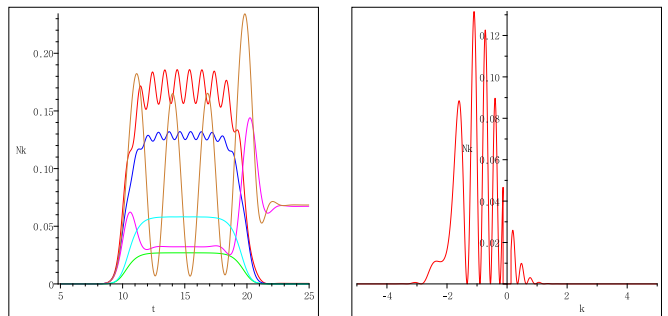


FIG. 12: (color online). The number of pairs $N_k(t)$ in the di-polarity Sauter electric field is plotted as a function of time for $k_{\parallel} = 1$ (red), $k_{\parallel} = 1.5$ (blue), $k_{\parallel} = 5$ (green), $k_{\parallel} = -1$ (magenta), $k_{\parallel} = -1.5$ (gold), and $k_{\parallel} = -5$ (skyblue) [left panel] and the longitudinal momentum spectrum is plotted at $t = 100$ [right panel].

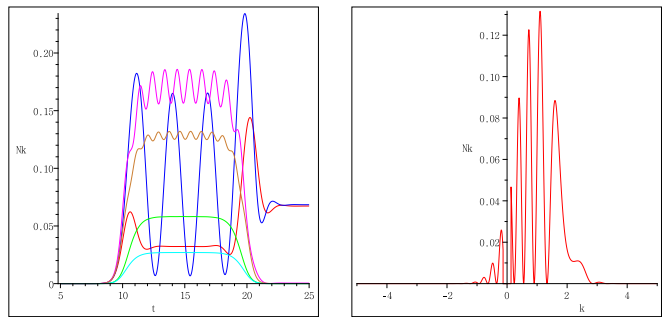


FIG. 13: (color online). The number of pairs $N_k(t)$ in $E(t) = -\frac{1}{\cosh^2(t-10)} + \frac{1}{\cosh^2(t-20)}$ is plotted as a function of time for $k_{\parallel} = 1$ (red), $k_{\parallel} = 1.5$ (blue), $k_{\parallel} = 5$ (green), $k_{\parallel} = -1$ (magenta), $k_{\parallel} = -1.5$ (gold), and $k_{\parallel} = -5$ (skyblue) [left panel] and the longitudinal momentum spectrum is plotted at $t = 100$ [right panel].

$m = 1$ in the Compton unit is equivalent to five wavelengths of a particle in ten Compton length width of the square barrier in the scattering picture IV and has the zero reflection coefficient due to resonance.

The effect of the polarity of the electric field can be seen in the right panel of Fig. 12 and Fig. 13, in which the longitudinal momentum spectrum shows the mirror symmetry when the polarity of the electric field changes. There are residual pairs with negative momentum (Fig. 12) when the first Sauter field acts in the positive direction and then the second one in the negative direction, while more pairs with positive momentum survive (Fig. 13) when the first Sauter field acts in the negative direction and then the second one in the positive direction. The number of pairs in time also shows the polarity effect as shown in the left panel of Fig. 12 and Fig. 13.

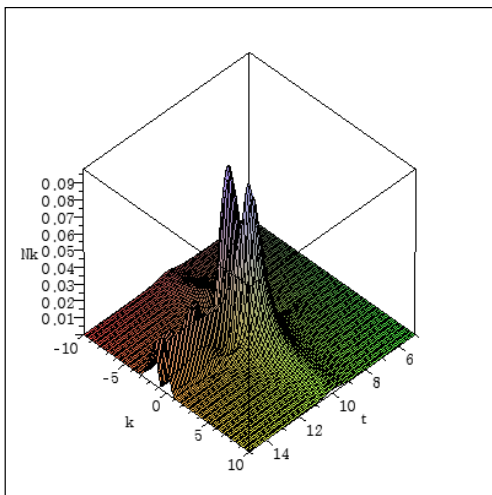


FIG. 14: (color online). The number of pairs in the inverse square potential is plotted as a function of time and longitudinal momentum.

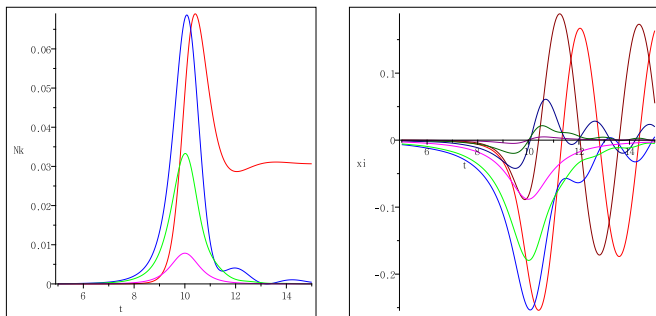


FIG. 15: (color online). For the inverse square potential, the number of pairs $N_k(t)$ [left panel] and the real and imaginary part of the function $\xi_k(t)$ [right panel] are plotted as a function of time for $k_{\parallel} = 0$ (red), $k_{\parallel} = 1$ (blue), $k_{\parallel} = 2$ (green), and $k_{\parallel} = 5$ (magenta).

$$\text{B. } A_{\parallel}(t) = \frac{E_0 \tau}{1 + \frac{t^2}{\tau^2}}$$

The inverse square potential shares the same property of vanishing in the remote past and future and changing polarity as the di-polarity Sauter electric field in Sec. VIA. The structure of the longitudinal momentum spectrum of pairs in the inverse square potential was discovered and explained as a consequence of Stokes phenomenon by Dumlu and Dunne [16, 17].

For the numerical work we set $E_0 = 1$ and $\tau = 1$. The peak of the number of pairs in Fig. 14 is relatively small compared with the Sauter or Gaussian electric field almost with the same peak intensity. Also it is small even compared with the di-polarity Sauter electric field. After the completion of interaction the number of pairs oscillates with small amplitude as shown in Fig. 15. The structure of the longitudinal momentum spectrum is shown in Fig. 16. The relatively simple looking spectrum has also a fine substructure as shown in the right panel

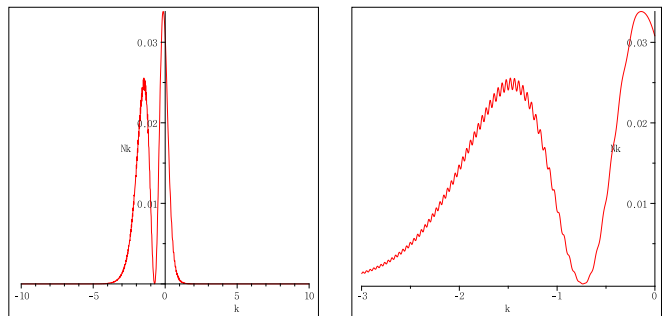


FIG. 16: (color online). For the inverse square potential, the longitudinal momentum spectrum of pairs at $t = 100$ is plotted as a function of parallel momentum in the range of $-10 \leq k_{\parallel} \leq 10$ [left panel] and the detailed plot $-3 \leq k_{\parallel} \leq 0$ [right panel].

of Fig. 16. The result of this section cannot be directly compared with that in Ref. [16, 17], in which the structure was found for a subcritical strength and longer time scale than ours in the Compton scale.

$$\text{C. } A_{\parallel}(t) = \frac{\sqrt{E_0(E_0+1)}\tau}{\cosh(\frac{t}{\tau})}$$

The solitonic gauge potential has a special energy condition

$$\omega^2(t) = \omega^2(-\infty) + \frac{n(n+1)\omega^2(-\infty)}{\cosh^2(\omega(-\infty)t)}, \quad (58)$$

where n is a natural number and $\omega(-\infty)$ is the Minkowski energy of particle in the remote past. The one-soliton ($n = 1$) and multi-soliton ($n = 2, \dots$) gauge fields correspond to soliton solutions for the inverse scattering of the Korteweg-de Vries (KdV) equation [36, 42]. The solitonic gauge potential is interesting in understanding the peculiarity of Schwinger mechanism by pulsed electric fields. Among the gauge potentials that vanish in the remote past and future, the solitonic gauge potential is unique in that the number of pairs produced by the corresponding electric field exponentially increases from and then decreases to zero [36, 42]. In fact, any gauge potential which has the reflectionless scattering for the field equation (36) has zero number of pairs in the remote future and may belong to the solitonic gauge potential.

For the numerical purpose, we consider the electric field with the center shifted

$$E(t) = \frac{\sqrt{E_0(E_0+1)} \sinh(\frac{t-10\tau}{\tau})}{\cosh^2(\frac{t-10\tau}{\tau})}, \quad (59)$$

and set $\tau = 1$ but select a natural number and non-natural number for the strength E_0 . The left panel of Fig. 17 is the number of pairs as a function of time for the solitonic gauge potentials $E_0 = 1, 2, 5$ and 10. The number of pairs increases and then decreases in symmetric way around the center $t = 10$ of the gauge potential

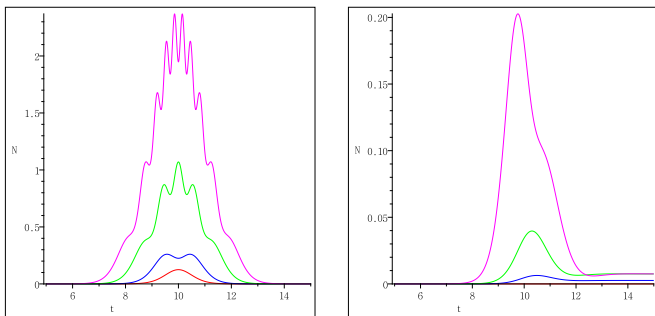


FIG. 17: (color online). The number of pairs $N(t)$ is plotted for the solitonic gauge potential with $E_0 = 1, 2, 5, 10$ [left panel] and for non-solitonic gauge potential with $E_0 = 0.2, 0.5, 1.5$ [right panel].

and the number of local maxima is the same as the soliton number [42]. On the other hand, for a non-natural number, for instance, $E_0 = 0.2, 0.5$ and 1.5 , the number of produced pairs increases from zero but decreases to a constant value. This temporal behavior of the number of pairs is expected from the asymptotic solutions (32) for $\omega(-\infty) = \omega(\infty)$ regardless of E_0 . It should be recollected that the inverse square potential has also finite number of pairs in the remote future in Sec. VI B, in contrast to the solitonic gauge field.

VII. DISCUSSION AND CONCLUSION

We have employed the evolution operator formalism to numerically study pair production in scalar QED by pulsed electric fields. The pulsed electric field is nontrivial in that it acts for a finite period of time and has the inhomogeneity of time. The Hamiltonian for a spinless charged boson in time-dependent electric field is an infinite sum of oscillators with time-dependent frequencies. After expressing the oscillator Hamiltonian in terms of the creation and annihilation operators of particle and antiparticle in the Minkowski vacuum, the evolution operator (14) in $SU(1, 1)$ algebra is factorized into the pair annihilation part, the number part and the pair creation part. The advantage of this factorization is that the exact quantum state (16) from the Minkowski vacuum under the influence of a pulsed electric field is the squeezed vacuum of particle and antiparticle with a complex phase factor. The sum of all complex time-dependent phase factors for the number operator determines the vacuum polarization and the vacuum persistence, which in turn is related to the number of pairs produced by the pulsed electric field.

Now the time-dependent Schrödinger equation is equivalent to a set of first order differential equations for the complex parameters for the evolution operator. The evolution of the Minkowski vacuum is governed by three parameters in Eqs. (23)-(25), and thus the set of first order differential equations can implement numerical works

for pair production in various configurations of the electric fields. Remarkably the differential equations have the asymptotic solutions (32) when the gauge potential vanishes and another solutions (33) when the gauge potential approaches a constant value. These asymptotic solutions put a strong constraint on the behavior of number of pairs such that the number of pairs per unit volume and per unit time is a constant for the zero-gauge potential in the remote future but it oscillates around the time-averaged value for a non-zero gauge potential.

For numerical works we have selected two classes of electric fields or gauge potentials. In the first class the electric field does not change the polarity of the field. Therefore, the gauge potential, as the negative of the time integral of electric field, should have a non-zero value in the remote future. We have considered (i) Sauter electric field, (ii) Gaussian electric field and (iii) oscillating Gaussian gauge potential as the first class of monopolarity electric field. In the second class the electric field changes the polarity and has the gauge potential which vanishes in the remote future. We have considered in the second class (iv) di-polarity Sauter electric field, two Sauter fields separated by a time gap, (v) inverse square gauge potential and (vi) solitonic gauge potential, all of which have the di-polarity of field.

We have computed the number of pairs as a function of time and longitudinal momentum for the pulsed electric fields of (i)-(vi) with the Compton scale. In the first class (i)-(iii), the number of pairs increases when the field acts and then oscillates around the time-averaged value as predicted by the asymptotic solutions. In general the number of pairs is suppressed for large longitudinal momentum as expected from the field equation in Sec. IV. The structure of longitudinal momentum spectrum is found for small momentum for (i)-(iii). Hebenstreit et al found the substructure of the spectrum in a sinusoidal electric field with Gaussian envelope [21] while the sinusoidal gauge potential is considered in this paper. Also, the structure of the momentum spectrum has been found for the class (v) by Dumlu and Dunne [16, 17]. The number of pairs as a function time or a function of momentum shows similarity between the Sauter electric field and the Gaussian electric field. However, the momentum spectrum for the oscillating Gaussian electric field reorganizes and bunches around one positive and one negative momenta with the same magnitude and the separation in the momentum space equals to the angular frequency of the oscillating electric field. We do not have a simple physical explanation for this bunching effect due to the oscillating field with a Gaussian envelope.

In the second class of di-polarity field (iv)-(vi) in which the gauge potential vanishes in the remote future, the number of pairs increases and then decreases to a constant rate and has relatively simpler structure of the longitudinal momentum than mono-polarity electric fields. Still the longitudinal momentum spectrum for the di-polarity Sauter electric field exhibits a surprising feature of negative or positive momentum dominance of

produced pairs depending on whether the positively directed pulse or the negatively directed pulse acts first, which is then followed by the oppositely directed second pulse. Further the solitonic gauge potential produces pairs in a symmetric way in time and returns back to the Minkowski vacuum without any residual pairs.

In this paper we have confined our study to scalar QED in pulsed electric fields. However, there are a few issues related to but not treated in this paper. First, the evolution operator formalism can also apply to spinor QED, since the spin-1/2 fermions have $SU(2)$ algebra isomorphic to $SU(1, 1)$ and may have an evolution operator similar to the spinless boson. Another issue is the vacuum polarization, the real part of the in- and the out-vacua scattering amplitude. To get a finite effective action one should properly regularize the sum over the momentum of the real part of the scattering amplitude. Still another issue is the back reaction of produced pairs. The strong field investigated in this paper produces roughly one pair per unit Compton volume, which could generate an induced electric field screening the external field and cause another mechanism for the oscillation of produced pairs [29, 30]. Finally, it would be extremely useful and promising for ELI experimentation to have a simi-

lar evolution operator formalism for both spatially and temporally localized electric fields. All these issues go beyond the scope of this paper and will be addressed in future publication.

Acknowledgments

S. P. K. and H. W. L. would like to thank Professor Remo Ruffini for the warm hospitality at ICRANet where this paper was completed. The work of S. P. K. was supported in part by Basic Science Research Program through the National Research Foundation of Korea (NRF) funded by the Ministry of Education, Science and Technology (22012R1A1B3002852). The work of H. W. L. was supported in part by the International Research and Development Program of the National Research Foundation of Korea (NRF) funded by the Ministry of Education, Science and Technology (MEST) of Korea(K21003002081-12B1200-00310). The work of R. R. was supported in part by ICRANet. The visit to ICRANet by S. P. K. and H. W. L. was supported in part by ICRA.

-
- [1] A. Ringwald, "Pair production from vacuum at the focus of an X-ray free electron laser," *Phys. Lett. B* **510**, 107 (2001) [hep-ph/0103185].
 - [2] R. Alkofer, M. B. Hecht, C. D. Roberts, S. M. Schmidt, and D. V. Vinnik, "Pair creation and an x-ray free electron laser," *Phys. Rev. Lett.* **87**, 193902 (2001) [nucl-th/0108046].
 - [3] D. B. Blaschke, A. V. Prozorkevich, C. D. Roberts, S. M. Schmidt, and S. A. Smolyansky, "Pair production and optical lasers," *Phys. Rev. Lett.* **96**, 140402 (2006) [nucl-th/0511085].
 - [4] S. S. Bulanov, V. D. Mur, N. B. Narozhny, J. Nees, and V. S. Popov, "Multiple colliding electromagnetic pulses: a way to lower the threshold of e+e- pair production from vacuum," *Phys. Rev. Lett.* **104**, 220404 (2010) [arXiv:1003.2623].
 - [5] G. V. Dunne, "New Strong-Field QED Effects at ELI: Nonperturbative Vacuum Pair Production," *Eur. Phys. J. D* **55**, 327 (2009) [arXiv:0812.3163].
 - [6] D. B. Blaschke, A. V. Prozorkevich, G. Ropke, C. D. Roberts, S. M. Schmidt, D. S. Shkirmanov, and S. A. Smolyansky, "Dynamical Schwinger effect and high-intensity lasers. Realising nonperturbative QED," *Eur. Phys. J. D* **55**, 341 (2009) [arXiv:0811.3570].
 - [7] A. Di Piazza, C. Müller, K. Z. Hatsagortsyan, and C. H. Keitel, "Extremely high-intensity laser interactions with fundamental quantum systems," to be published in *Rev. Mod. Phys.* [arXiv:1111.3886].
 - [8] E. Brezin and C. Itzykson, "Pair Production in Vacuum by an Alternating Field," *Phys. Rev. D* **2**, 1191 (1970).
 - [9] V. S. Popov, "Pair Production in a variable external field (quasiclassical approximation)," *Sov. Phys. JETP* **34**, 709 (1972).
 - [10] V. S. Popov, "Tunnel and multiphoton ionization of atoms and ions in a strong laser field (Keldysh theory)," *Phys.-Usp.* **47**, 855 (2004).
 - [11] G. V. Dunne and C. Schubert, "Worldline instantons and pair production in inhomogeneous fields," *Phys. Rev. D* **72**, 105004 (2005) [arXiv:hep-th/0507174].
 - [12] G. V. Dunne, Q.-H. Wang, H. Gies, and C. Schubert, "Worldline instantons and the fluctuation prefactor," *Phys. Rev. D* **73**, 065028 (2006) [arXiv:hep-th/0602176].
 - [13] S. P. Kim and D. N. Page, "Schwinger pair production via instantons in a strong electric field," *Phys. Rev. D* **65**, 105002 (2002) [arXiv:hep-th/0005078].
 - [14] S. P. Kim and D. N. Page, "Improved approximations for fermion pair production in inhomogeneous electric fields," *Phys. Rev. D* **75**, 045013 (2007) [arXiv:hep-th/0701047].
 - [15] H. Kleinert, R. Ruffini, and S.-S. Xue, "Electron-positron pair production in space- or time-dependent electric fields," *Phys. Rev. D* **78**, 025011 (2008) [arXiv:0807.0909].
 - [16] C. K. Dumlu and G. V. Dunne, "The Stokes Phenomenon and Schwinger Vacuum Pair Production in Time-Dependent Laser Pulses," *Phys. Rev. Lett.* **104**, 250402 (2010) [arXiv:1004.2509].
 - [17] C. K. Dumlu and G. V. Dunne, "Interference effects in Schwinger vacuum pair production for time-dependent laser pulses," *Phys. Rev. D* **83**, 065028 (2011) [arXiv:1102.2899].
 - [18] C. K. Dumlu and G. V. Dunne, "Complex worldline instantons and quantum interference in vacuum pair production," *Phys. Rev. D* **84**, 125023 (2011) [arXiv:1110.1657].
 - [19] R. Schützhold, H. Gies, and G. Dunne, "Dynamically

- assisted Schwinger mechanism,” *Phys. Rev. Lett.* **101**, 130404 (2008) [arXiv:0807.0754].
- [20] F. Hebenstreit, R. Alkofer and H. Gies, “Pair production beyond the Schwinger formula in time-dependent electric fields,” *Phys. Rev. D* **78**, 061701 (2008) [arXiv:0807.2785].
- [21] F. Hebenstreit, R. Alkofer, G. V. Dunne, and H. Gies, “Momentum signatures for Schwinger pair production in short laser pulses with sub-cycle structure,” *Phys. Rev. Lett.* **102**, 150404 (2009) [arXiv:0901.2631].
- [22] C. K. Dumlu, “On the quantum kinetic approach and the scattering approach to vacuum pair production,” *Phys. Rev. D* **79**, 065027 (2009) [arXiv:0901.2972].
- [23] A. Di Piazza, E. Lotstedt, A. I. Milstein, and C. H. Keitel, “Barrier control in tunneling e+e photoproduction,” *Phys. Rev. Lett.* **103**, 170403 (2009) [arXiv:0906.0726].
- [24] G. V. Dunne, H. Gies, and R. Schützhold, “Catalysis of Schwinger vacuum pair production,” *Phys. Rev. D* **80**, 111301 (2009) [arXiv:0908.0948].
- [25] C. K. Dumlu, “Schwinger Vacuum Pair Production in Chirped Laser Pulses,” *Phys. Rev. D* **82**, 045007 (2010) [arXiv:1006.3882].
- [26] F. Hebenstreit, R. Alkofer, and H. Gies, “Schwinger pair production in space and time-dependent electric fields: Relating the Wigner formalism to quantum kinetic theory,” *Phys. Rev. D* **82**, 105026 (2010) [arXiv:1007.1099].
- [27] M. Orthaber, F. Hebenstreit, and R. Alkofer, “Momentum Spectra for Dynamically Assisted Schwinger Pair Production,” *Phys. Lett. B* **698**, 80-85 (2011) [arXiv:1102.2182].
- [28] F. Hebenstreit, R. Alkofer, and H. Gies, “Particle self-bunching in the Schwinger effect in spacetime-dependent electric fields,” *Phys. Rev. Lett.* **107**, 180403 (2011) [arXiv:1106.6175].
- [29] Y. Kluger, J. M. Eisenberg, B. Svetitsky, F. Cooper, and E. Mottola, “Pair production in a strong electric field,” *Phys. Rev. Lett.* **67**, 2427 (1991).
- [30] Y. Kluger, J. M. Eisenberg, B. Svetitsky, F. Cooper, and E. Mottola, “Fermion pair production in a strong electric field,” *Phys. Rev. D* **45**, 4659 (1992).
- [31] S. A. Smolyansky, G. Ropke, S. M. Schmidt, D. Blaschke, V. D. Toneev, and A. V. Prozorkevich, “Dynamical derivation of a quantum kinetic equation for particle production in the Schwinger mechanism,” [hep-ph/9712377].
- [32] Y. Kluger, E. Mottola, and J. M. Eisenberg, “The Quantum Vlasov equation and its Markov limit,” *Phys. Rev. D* **58**, 125015 (1998) [hep-ph/9803372].
- [33] S. M. Schmidt, D. Blaschke, G. Ropke, S. A. Smolyansky, A. V. Prozorkevich, and V. D. Toneev, “A Quantum kinetic equation for particle production in the Schwinger mechanism,” *Int. J. Mod. Phys. E* **7**, 709 (1998) [hep-ph/9809227].
- [34] V. N. Pervushin, V. V. Skokov, A. V. Reichel, S. A. Smolyansky, and A. V. Prozorkevich, “The Kinetic description of vacuum particle creation in the oscillator representation,” *Int. J. Mod. Phys. A* **20**, 5689 (2005) [hep-th/0307200].
- [35] A. M. Fedotov, E. G. Gelfer, K. Y. Korolev, and S. A. Smolyansky, “On the kinetic equation approach to pair production by time-dependent electric field,” *Phys. Rev. D* **83**, 025011 (2011) [arXiv:1008.2098].
- [36] S. P. Kim and C. Schubert, “Nonadiabatic quantum Vlasov equation for Schwinger pair production,” *Phys. Rev. D* **84**, 125028 (2011) [arXiv:1110.0900].
- [37] C. F. Lo, “Generating displaced and squeezed number states by a general driven time-dependent oscillator,” *Phys. Rev. A* **43**, 404 (1991).
- [38] A. B. Balantekin and S. H. Fricke, “Interference effects in the Schwinger pair-production mechanism,” *Phys. Rev. D* **43**, 250 (1991).
- [39] A. B. Balantekin, J. E. Seger, and S. H. Fricke, “Dynamical Effects in Pair Production by Electric Fields,” *Int. J. Mod. Phys. A* **6**, 695 (1991).
- [40] S. P. Kim, H. K. Lee and Y. Yoon, “Effective action of QED in electric Field backgrounds,” *Phys. Rev. D* **78**, 105013 (2008) [arXiv:0807.2696].
- [41] A. I. Nikishov, “Barrier scattering in field theory removal of Klein paradox,” *Nucl. Phys. B* **21**, 346 (1970)
- [42] S. P. Kim, “Schwinger Pair Production in Solitonic Gauge Fields,” [arXiv:1110.4684].